phys. stat. sol. (c) **6**, No. 1, 162–167 (2009) / **DOI** 10.1002/pssc.200879834

physica status solidi c
www.pss-c.com
current topics in solid state physics

Exciton coherence in semiconductor quantum dots

Junko Ishi-Hayase[1,2,3*], Kouichi Akahane[2], Naokatsu Yamamoto[2], Mamiko Kujiraoka[2,4], Kazuhiro Ema[4], and Masahide Sasaki[2]

[1] PRESTO, Japan Science and Technology Agency (JST), 4-1-8 Honcho, Kawaguchi, Saitama 332-0012, Japan
[2] National Institute of Information and Communications Technology (NICT), 4-2-1 Nukui-Kitamachi, Koganei, Tokyo 184-8795, Japan
[3] The Education and Research Center for Frontier Science and Engineering, The University of Electro-Communications, 1-5-1 Chofu-ga-oka, Chofu, Tokyo 182-8585, Japan
[4] Department of Physics, Sophia University, 7-1 Kioicho, Chiyoda-ku, Tokyo 102-8554, Japan

Received 17 June 2008, revised 25 July 2008, accepted 30 July 2008
Published online 30 September 2008

PACS 71.35.-y, 78.47.jf, 78.47.nj, 78.67.Hc

* Corresponding author: e-mail j-hayase@nict.go.jp, Phone: +81-42-327-7046, Fax: +81-42-327-6629

The coherent dynamics of excitons in InAs quantum dots (QDs) was investigated in the telecommunication wavelength range using a transient four-wave mixing technique. The sample was fabricated on an InP(311)B substrate using strain compensation to control the emission wavelength. This technique also enabled us to fabricate a 150-layer stacked QD structure for obtaining a high S/N in the four-wave mixing measurements, although no high-sensitive heterodyne detection was carried out. The dephasing time and transition dipole moment were precisely estimated from the polarization dependence of signals, taking into account their anisotropic properties. The population lifetimes of the excitons were also measured by using a polarization-dependent pump-probe technique. A quantitative comparison of these anisotropies demonstrates that in our QDs, non-radiative population relaxation, polarization relaxation and pure dephasing are considerably smaller than the radiative relaxation. A comparison of the results of the four-wave mixing and pump-probe measurements revealed that the pure dephasing could be directly estimated with an accuracy of greater than 0.1 μeV by comparing the results of four-wave mixing and pump-probe measurements.

1 Introduction The coherent dynamics and manipulation of excitons in self-assembled quantum dots (SAQDs) have been key issues in the implementation of quantum information processing and quantum communications [1,2]. SAQDs that emit light at telecommunication wavelengths have attracted significant interest because of their possible applications in long-distance optical [3] and quantum communications [4,5]. Hence, fabrication techniques such as strain compensation [5–7] and the double-cap method [7,8] have been developed to redshift the emission wavelength of SAQDs. Recently, some research groups have reported the advantages of strain-compensated InAs SAQDs grown on an InP(311)B substrate [6,7,9,10]. These advantages include long-wavelength emission and realization of a multilayer stacked structure without defects and imperfections. Owing to the orientation of (311)B substrates, SAQDs grown on an InP(311)B substrate should exhibit optical anisotropy, which is analogous to that exhibited for quantum wells grown on a (311)B substrate [11]. Optical anisotropy is expected to affect the coherent and population dynamics of excitons. For investigating these dynamics, we must perform polarization-sensitive transient nonlinear spectroscopies, such as four-wave mixing (FWM) and pump-probe (PP) spectroscopies, under resonant excitation of the exciton ground states. However, it is difficult to apply these techniques to QDs when the signal intensity is weak owing to a low QD density. Hence, to enhance the nonlinear signals, we used a multilayer stacked structure of strain-compensated SAQDs to enhance nonlinear signals [12,13].

In this paper, we report the investigation of the coherent and population dynamics of excitons using transient FWM and PP spectroscopic techniques under resonant excitation in the telecommunication wavelength range. InAs

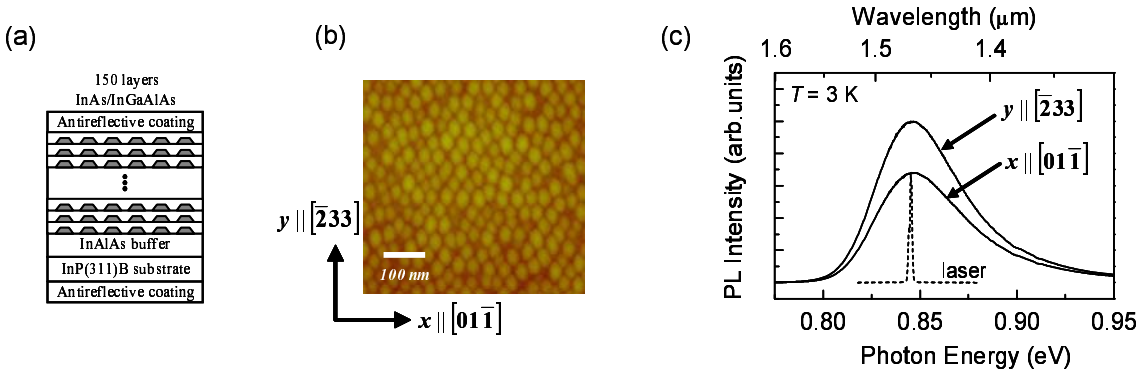

Figure 1 (a) Schematic of our sample structure. (b) AFM image of topmost (150th) QD layer. (c) Photoluminescence spectra for $\boldsymbol{x}$ and $\boldsymbol{y}$ polarizations at 3 K under nonresonant laser excitation (solid lines). Exciton ground state emission peaks at the wavelength of 1.468 μm. The dashed line represents the spectrum of the incident pulses used in the FWM and PP spectroscopies.

SAQDs grown on an InP(311)B substrate using strain compensation were used as the sample. Polarization-sensitive measurements enabled us to estimate the individual exciton lifetimes and dephasing times for two orthogonally polarized ground states of the excitons [14].

2 Experimentals The sample consists of 150 layers of InAs SAQDs embedded in 60-nm-thick $In_{0.52}Ga_{0.1}Al_{0.38}As$ spacers grown on an InP(311)B substrate, as shown in Fig. 1(a). Molecular beam epitaxy was used for the sample growth [6,9]. By precise control of the composition of the spacers and by using an InP(311)B substrate, we made the QD strain smaller than that observed in ordinary In(Ga)As/GaAs SAQDs grown on a GaAs substrate. This strain compensation enabled us to shift the emission wavelength of the QDs to the telecommunication wavelengths. Additionally, strain compensation enabled us to stack more than a hundred QD layers, which helped in enhancing weak nonlinear signals. Figure 1(b) shows an atomic force microscopy (AFM) image of the topmost (150th) layer in the QD stack. The average lateral size of the QDs was estimated to be 51 nm in the $[\bar{2}33]$ direction and 39 nm in the $[01\bar{1}]$ direction. The area density of the QDs in the topmost layer was approximately $9 \times 10^{10}/\mathrm{cm}^2/\mathrm{layer}$.

Figure 1(c) shows the photoluminescence spectra measured at 3 K under non-resonant excitation for different polarization directions. The exciton ground-state emissions reached a maximum intensity at 1.468 μm for both polarization directions. The ground state and first-excited state of the excitons were separated by 53 meV. This energy separation was found to be sufficiently larger than the inhomogeneous broadening of the transition energies (HWHM $\sim$ 22 meV). The photoluminescence intensity changes with the polarization direction as can be clearly seen in Fig. 1(c). The polarization dependence is attributed to the anisotropy of the QD shape, QD composition, QD strain and the atomistic asymmetry of the crystal [15]. As already discussed in the literature, these anisotropies lift the degeneracy of the exciton ground states. Hence, the exciton ground states of our QDs are split into orthogonally polarized states in the $[01\bar{1}]$ ($\boldsymbol{x}$) and $[\bar{2}33]$ ($\boldsymbol{y}$) direction. In this study, we use $|x\rangle$ and $|y\rangle$ to represent the $\boldsymbol{x}-$ and $\boldsymbol{y}-$polarized states, respectively.

The time evolution of exciton coherence and population was measured using transient FWM and PP techniques. All the measurements were performed using 1.1-ps optical pulses (repetition rate: 76 MHz) generated from an optical parametric oscillator pumped by a mode-locked Ti:sapphire laser. The dashed line in Fig. 1(c) indicates the spectrum of the incident pulses. The wavelength of the incident pulses was tuned to 1.468 μm to excite the ground-state excitons resonantly. The polarization directions of the linearly polarized incident pulses were controlled using half-wave plates to investigate the polarization dependences of the FWM and PP signals. The polarization selection rules allowed us to selectively excite either the $|x\rangle$ or $|y\rangle$ states. In this paper, the angle between the polarization direction of the incident pulses and the $[01\bar{1}]$ direction is represented as θ. The sample was maintained at 3 K for all the measurements.

The FWM experiment was performed using the two-pulse self-diffraction configuration to measure the dephasing time T_2 of excitons. A schematic image of the experimental setup is shown in the inset of Fig. 2(a). The time-integrated FWM signal intensity in the $2\boldsymbol{k}_2 - \boldsymbol{k}_1$ direction was measured as a function of the time delay τ between two excitation pulses. The $\boldsymbol{k}_1$ and $\boldsymbol{k}_2$ pulses had parallel polarizations. The intensities of the excitation pulses were adjusted to 16 kW/cm^2; at this intensity, no significant excitation dependence of T_2 was observed. A PP experiment was performed in the transmission geometry to investigate the population dynamics of the excitons. The differential transmission (DT) of the probe pulse was detected for various τ values between the pump and probe pulses. The in-

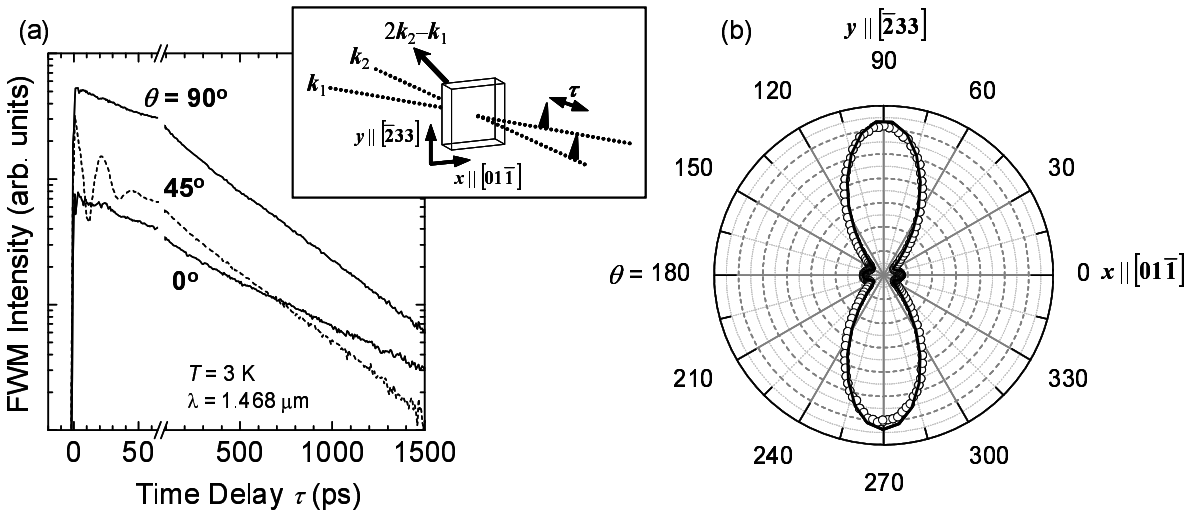

Figure 2 (a) FWM intensities vs time delay, τ, for various polarization directions of incident pulses. θ represents the angle between the polarization direction of incident pulses and the $[01\bar{1}]$ direction. (inset) An experimental setup of FWM spectroscopy. (b) FWM intensities for $\tau = 200$ ps measured as a function of θ. The experimental results were well reproduced by the theoretical curve (solid line) calculated using the equation $E_0^6 * (|\mu^x|^8 \cos^6\theta \exp(-4\tau/T_2^x) + |\mu^y|^8 \sin^6\theta \exp(-4\tau/T_2^y))$.

tensity of the pump pulse was the same as that used in the FWM experiment, and the intensity of the probe pulse was 0.5% of that of the pump pulse.

3 Results and discussion

3.1 Four-wave mixing spectroscopy Figure 2(a) shows typical FWM signals for various polarization directions, θ. At $\tau < 60$ ps, a beat signal was observed only for $\theta = 45$ °, where the $|x\rangle$ and $|y\rangle$ states were simultaneously excited. Thus, the beat signal resulted from the coherent superposition between the $\boldsymbol{x}-$ and the $\boldsymbol{y}-$polarized transitions. This is well known as a fine-structure quantum beat [16]. The period of the beat was estimated to be 23 ps, which corresponds to a splitting energy of 180 μeV. The quantum beat almost vanished for $\theta = 0$ ° and 90 °. This clearly proves the polarization selection rules with respect to $|0\rangle - |x\rangle$ and $|0\rangle - |y\rangle$ transitions.

For a long τ, the observed FWM signal decayed exponentially with a large time constant, indicating the long dephasing time of the excitons in the QDs. The decay time constants and signal intensities of the slow component were clearly different for $\boldsymbol{x}$ and $\boldsymbol{y}$ polarizations. The anisotropy of the decay time indicates that the T_2 values for the $\boldsymbol{x}-$ and $\boldsymbol{y}-$polarized transitions significantly differ from each other. We estimated the T_2 values to be $T_2^x = 2.86$ ns for the $\boldsymbol{x}-$polarized transition and $T_2^y = 1.64$ ns for the $\boldsymbol{y}-$polarized transition [13]. The T_2^x value is larger than any other T_2 value reported for QD excitons so far [1, 17–20]. Using the equation $\gamma_h = 2\hbar/T_2$, we calculated the homogeneous broadenings of the zero-phonon lines γ_h to be $\gamma_h^x = 0.46 \pm 0.01$ μeV and $\gamma_h^y = 0.80 \pm 0.01$ μeV.

The polarization dependence of the FWM signal intensity is related to the anisotropy of the transition dipole moment $|\mu|$ for the $\boldsymbol{x}-$ and the $\boldsymbol{y}-$polarized transitions because an FWM signal intensity is proportional to $|\mu|^8$. Figure 2(b) shows the FWM intensities for $\tau = 200$ ps measured in various polarization directions, θ, of the incident pulses at the same incident intensities. In general, an FWM intensity is proportional to $E^6|\mu|^8 \exp(-4\tau/T_2)$, where E represents the amplitude of the incident electric field [21]. The FWM intensity at θ should be the sum of the FWM intensities associated with the $\boldsymbol{x}-$ and the $\boldsymbol{y}-$polarized transitions. Based on the abovementioned interpretation, the FWM intensity at θ is represented by the equation $E_0^6 * (|\mu^x|^8 \cos^6\theta \exp(-4\tau/T_2^x) + |\mu^y|^8 \sin^6\theta \exp(-4\tau/T_2^y))$. The theoretical curve calculated by the equation is in excellent agreement with the experimental data shown in Fig. 2(b). In the calculation, we used the values of T_2^x and T_2^y estimated from the decay time constants of the FWM intensity. Consequently, the ratio of $|\mu|^2$ for $\boldsymbol{x}-$ and $\boldsymbol{y}-$polarized transitions was estimated to be $|\mu^x/\mu^y|^{-2} = 1.72 \pm 0.04$.

This ratio coincides with the ratio of $T_2^x/T_2^y = 1.75 \pm 0.07$. This agreement implies that T_2 are dominated by the radiative lifetimes, T_r, because T_r is proportional to $|\mu|^{-2}$. In other words, both dephasing due to non-radiative population relaxation and pure dephasing without population relaxation are very small [19]. A similar analysis was performed by W. Langbein et al. They also found a radiatively limited T_2 in InAs/GaAs QDs grown on a GaAs(100) substrate at shorter wavelengths [19] compared to that used in this study. Table 1 shows the comparison of T_2 and other parameters obtained for the QDs investigated by W. Lang-

bein et al. using the polarization-dependent FWM method with those of our QDs. We found that the T_2^x for our QDs is longer than that for their QDs, while the T_2^ys are similar in both cases. This is due to the large anisotropy of $|\mu|$ in our QDs. One of the possible origins of the large anisotropy is the low symmetry of the high-index substrate [15]. Our result demonstrates that substrate orientation is one of effective factors that determine the anisotropy of $|\mu|$, i.e., a radiatively limited T_2.

Table 1 Dephasing time T_2 and other parameters for strain-compensated InAs QDs obtained from FWM measurements. For comparison, parameters of InAs QDs reported by W. Langbein et al. are summarized.

Parameters	Present work	Langbein's work [19]
QD/spacer	InAs/InGaAlAs	InAs/GaAs
substrate	InP(311)B	GaAs(100)
wavelength	1.468 μm	1.26 μm
crystal axes	$\boldsymbol{x} \parallel [01\bar{1}]$, $\boldsymbol{y} \parallel [\bar{2}33]$	$\boldsymbol{x} \parallel [110]$, $\boldsymbol{y} \parallel [1\bar{1}0]$
T_2^x (temp.)	2.86 ns (3 K)	2.1 ns (5 K)
T_2^y (temp.)	1.64 ns (3 K)	1.6 ns (5 K)
T_2^x/T_2^y	1.75 ± 0.07	1.316 ± 0.005
$\lvert\mu^x/\mu^y\rvert^{-2}$	1.72 ± 0.04	1.32 ± 0.015

3.2 Pump-probe spectroscopy For a more precise estimation of the radiative contribution to dephasing, we measured the absolute value of T_r by using a polarization-dependent PP technique. The time evolution of DT is determined only by the population dynamics of the excitons because we could ignore the effect of biexciton formation due to the narrow band and the weakness of the pump pulse. To analyse the DT decay rates, we considered the relaxation times shown in Fig. 3. $T_r^{x(y)}$ and $T_{nr}^{x(y)}$ represents the population decay times due to the radiative and non-radiative transitions from the $|x\rangle$ ($|y\rangle$) state to $|0\rangle$ state. T_{nr}^{xy} represents the polarization relaxation time between $|x\rangle$ and $|y\rangle$.

Figure 4(a) shows the DT at various τ for the $\boldsymbol{x}$ and $\boldsymbol{y}$ polarizations of the pump pulse. Adhering to the polarization selection rules, we selectively excited the exciton ground state that had the same polarization as the pump pulse at zero delay. The probe pulses were cross-linearly polarized with respect to the pump pulses. The DT profiles were well fitted by single exponential functions with different decay time constants. The DT decay times were determined to be t^x = 1.7 ns and t^y = 1.0 ns, which are clearly anisotropic.

The DT decay time is generally influenced not only by $T_r^{x(y)}$ but also by $T_{nr}^{x(y)}$ and T_{nr}^{xy}. To simplify the analysis of the experimental results, we independently estimated T_{nr}^{xy} by measuring the polarization degree. Figure 4(b) shows the time evolution of the polarization degree when the $\boldsymbol{y}-$polarized state is selectively excited by the pump pulse. The polarization degree did not change for $\tau < 1.5$ ns. From the exponential fitting of the polarization degree, T_{nr}^{xy} was found to be at least longer than several tens of nanoseconds. The value of T_{nr}^{xy} is considerably longer than the typical value of T_r, which is of the order of 1 ns. Therefore, the contribution of the polarization relaxation to the DT decay rates observed in Fig. 4(a) is negligible. In this case, the DT decay time in Fig. 4(a) is determined by $T_r^{x(y)}$ and $T_{nr}^{x(y)}$ of the exciton ground state that is selectively excited by the pump pulse. Since T_r is proportional to $|\mu|^{-2}$, the ratio T_r^x/T_r^y should be $|\mu^x/\mu^y|^{-2}$. The ratio $t^x/t^y = 1.7 \pm 0.2$ is in quantitative agreement with the ratio $|\mu^x/\mu^y|^{-2}$ estimated in the FWM measurements, within a margin of error. Therefore, the DT decay time should directly correspond to T_r, and for our QDs, the non-radiative population relaxation was found to be negligible compared with the radiative population relaxations. Thus, we conclude that T_r^x = 1.7 ns and T_r^y = 1.0 ns. This result clearly demonstrates the high crystalline nature of our QDs. This is one of the reasons why our QDs show a long T_2.

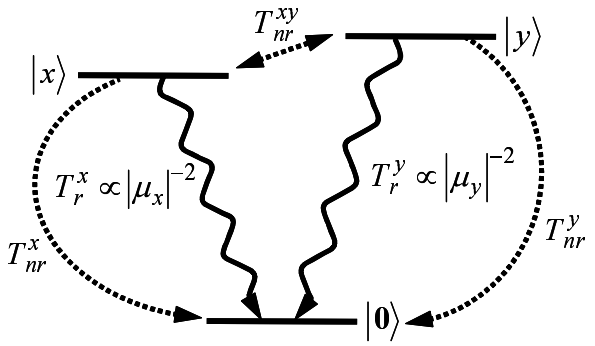

Figure 3 Energy-level diagram and optically allowed transitions related to exciton ground states in QD with broken rotational invariance. $|x\rangle$ and $|y\rangle$ correspond to the $\boldsymbol{x}-$ and $\boldsymbol{y}-$polarized states. The parameters in the diagram represent the relaxation times, as explained in the text.

The precise measurement of T_r enabled us to calculate the absolute value of $|\mu|$. $|\mu|^2$ can be determined using the equation [22]

$$|\mu|^2 = \left[\frac{9\epsilon^{5/2}}{(2\epsilon+\epsilon_{QD})^2}\frac{\omega^3}{3\pi\epsilon_0\hbar c_{vac}^3}\right]^{-1}\frac{1}{T_r}, \qquad (1)$$

where ϵ_{QD} and ϵ represent the dielectric constant for the QDs and their surrounding medium, respectively. The calculated values of $|\mu|^2$ are $|\mu^x|^2$ = 45 Debye and $|\mu^y|^2$ = 58 Debye. These values are larger than those reported for In(Ga)As SAQDs; that is, excitons in our SAQDs strongly interact with light. The values of $|\mu|^2$ were also found to be in good agreement with those estimated from the Rabi frequency, including their anisotropic characteristics [23].

This agreement demonstrates the high precision of the values of T_r measured by PP spectroscopy.

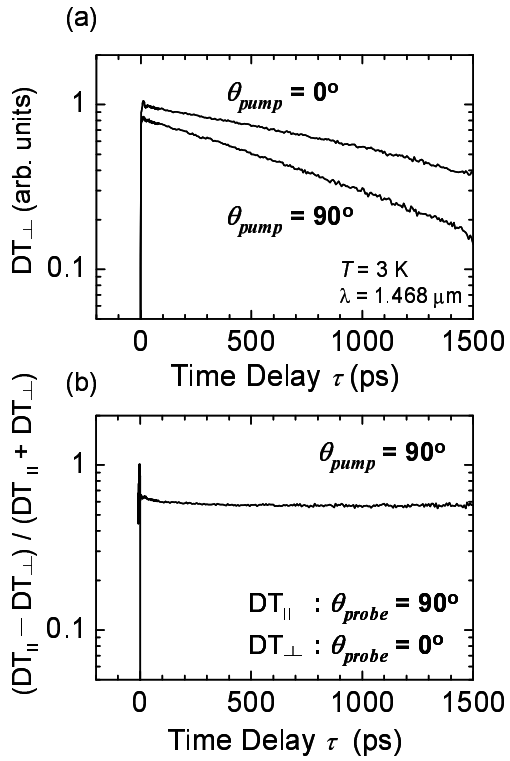

Figure 4 (a) DT of probe pulse at 3 K for θ_{pump} = 0 ° (x polarization) and θ_{pump} = 90 ° (y polarization). The probe pulses are cross-linearly polarized with respect to the pump pulses. (b) The time evolution of the polarization degree for θ_{pump} = 90 °.

3.3 Precise estimation of pure dephasing The simultaneous measurement of the FWM and PP signals enabled us to estimate pure dephasing, γ_{pure}, which causes dephasing without changing the exciton population. The relationship between γ_h, γ_r and γ_{pure} is expressed by the equation $\gamma_h = \gamma_r + \gamma_{pure}$ when the non-radiative population relaxation is negligible, as described in the previous subsection. γ_r represents the dephasing caused by the radiative population relaxation. From the results of PP spectroscopy, we calculated the radiative dephasing to be γ_r^x = 0.38 ± 0.01 μeV and γ_r^y = 0.65 ± 0.06 μeV using the relation $\gamma_r = \hbar/T_r$. These values are very close to those of γ_h. This confirms the conclusions made in the previous subsections, i.e. the dephasing is mainly caused by the radiative recombination process, and the pure dephasing is very small. By comparing γ_h with γ_r, we estimated the values of γ_{pure} to be γ_{pure}^x = 0.08 ± 0.02 μeV and γ_{pure}^y = 0.15 ± 0.07 μeV. Thus, the obtained γ_{pure} is considerably smaller than γ_r. This explains the long coherence times of the excitons in our QDs. γ_{pure} for our QDs is considerably smaller than the typical values for QDs reported in previous studies.

The error in the estimation of γ_{pure} is greater than 0.1 μeV, as described above, though the excitation intensity was weak and no high-sensitive heterodyne detection was performed. The estimation error is significantly smaller than that reported in earlier studies since in our FWM and PP measurements, we could achieve a high signal-to-noise ratio (S/N) by using a 150-layer-stacked structure of QDs [12]. Moreover, the simultaneous measurement of the FWM and PP signals with a high S/N afforded a greater accuracy in the determination of γ_{pure} than did the measurement of the FWM signals alone. The highly accurate measurement of γ_{pure} greatly assists the investigation of a pure dephasing mechanism, such as exciton-phonon interactions, which still remains a critical issue in physics of QDs. Temperature-dependent measurements of γ_{pure} will provide a detailed information on the pure dephasing mechanism, which will be published elsewhere.

4 Conclusions We performed transient FWM and PP spectroscopies to investigate the coherent and population dynamics of excitons in strain-compensated InAs SAQDs grown on an InP(311)B substrate. The emission wavelength of an exciton ground state was in the telecommunication wavelength range. The radiative lifetime and dephasing time exhibited large in-plane anisotropy due to the anisotropy of the transition dipole moment. The anisotropy of our QDs is larger than that of the QDs grown on a GaAs(100) substrate, which is due to the low symmetry of the high-index substrate employed in this study. The polarization dependence of the decay times of both the FWM and the PP signals is in quantitative agreement with the polarization dependence of the transition dipole moment. This shows that non-radiative population relaxation, polarization relaxation and pure dephasing are considerably smaller than radiative population relaxation. These results clearly indicate that our strain-compensated QDs have excellent optical properties. The simultaneous measurements of the FWM and PP signals with a high signal-to-noise ratio allowed us to directly measure the pure dephasing with an accuracy of greater than 0.1 μeV, which gives a powerful tool to investigate pure dephasing mechanism in QDs.

Acknowledgements This study was partially supported by a Grant-in-Aid for Scientific Research from the Ministry of Education, Culture, Sports, Science, and Technology of Japan. All the samples were fabricated at the Photonic Device Laboratory, NICT.

References

[1] P. Borri, W. Langbein, S. Schneider, U. Woggon, R. L. Sellin, D. Ouyang, and D. Bimberg, Phys. Rev. Lett. **87**, 157401 (2001).

[2] X. Li, Y. Wu, D. Steel, D. Gammon, T. H. Stievater, D. S. Katzer, D. Park, C. Piermarocchi, and L. J. Sham, Science **301**, 809 (2003).
[3] N. Yamamoto, K. Akahane, S. Gozu, and N. Ohtani, Appl. Phys. Lett. **86**, 203118 (2005).
[4] T. Miyazawa, K. Takemoto, Y. Sakuma, S. Hirose, T. Usuki, N. Yokoyama, M. Takatsu, and Y. Arakawa, Jpn. J. Appl. Phys. **44**, L620 (2005).
[5] M. B. Ward, O. Z. Karimov, D. C. Unitt, Z. L. Yuan, P. See, D. G. Gevaux, A. J. Shields, P. Atkinson, and D. A. Ritchie, Appl. Phys. Lett. **86**, 201111 (2005).
[6] K. Akahane, N. Ohtani, Y. Okada, and M. Kawabe, J. Cryst. Growth **245**, 31 (2002).
[7] C. Paranthoen, C. Platz, G. Moreau, N. Bertru, O. Dehaese, A. L. Corre, P. Miska, J. Even, H. Folliot, C. L. e, G. Patriarche, J. C. Simon, and S. Loualiche, J. Cryst. Growth **241**, 230 (2003).
[8] K. Takemoto, Y. Sakuma, S. Hirose, T. Usuki, and N. Yokoyama, Jpn. J. Appl. Phys. **43**, L349 (2004).
[9] K. Akahane, N. Yamamoto, S. Gozu, and N. Ohtani, Conference Proceedings of 16th International Conference on Indium Phosphide and Related Materials (IPRM'04) p. 85 (2004).
[10] C. Cornet, C. Labbe, H. Folliot, N. Bertru, O. Dehaese, J. Even, A. L. Corre, C. Paranthoen, C. Platz, and S. Loualiche, Appl. Phys. Lett. **85**, 5685 (2004).
[11] N. Nishiyama, M. Arai, S. Shinada, M. Azuchi, T. Miyamoto, F. Koyama, and K. Iga, IEEE J. Select. Topics Quantum Electron. **7**, 242 (2001).
[12] J. Ishi-Hayase, K. Akahane, N. Yamamoto, M. Sasaki, M. Kujiraoka, and K. Ema, Appl. Phys. Lett. **88**, 261907 (2006).
[13] J. Ishi-Hayase, K. Akahane, N. Yamamoto, M. Sasaki, M. Kujiraoka, and K. Ema, Appl. Phys. Lett. **91**, 103111 (2007).
[14] J. Ishi-Hayase, K. Akahane, N. Yamamoto, M. Sasaki, M. Kujiraoka, and K. Ema, J. Lumin. **119**/**120**, 318 (2006).
[15] S. Sanguinetti, S. Castiglioni, E. Grilli, M. Guzzi, G. Panzarini, L. C. Andreani, and M. Henini, Jpn. J. Appl. Phys. **38**, 4676 (1999).
[16] W. Langbein, P. Borri, and U. Woggon, Phys. Rev. B **69**, 161301(R) (2004).
[17] D. Birkedal, K. Leosson, and J. M. Hvam, Phys. Rev. Lett. **87**, 227401 (2001).
[18] M. Bayer and A. Forchel, Phys. Rev. **B 65**, 041308R (2002).
[19] W. Langbein, P. Borri, U. Woggon, V. Stavarache, D. Reuter, and A. K. Wieck, Phys. Rev. B **70**, 033301 (2004).
[20] P. Borri, W. Langbein, U. Woggon, V. Stavarache, D. Reuter, and A. K. Wieck, Phys. Rev. **B 71**, 115328 (2005).
[21] T. Yajima and Y. Taira, J. Phys. Soc. Jpn. **47**, 1620 (1979).
[22] A. Thränhardt, C. Ell, G. Khitrova, and H. M. Gibbs, Phys. Rev. B **65**, 035327 (2002).
[23] J. Ishi-Hayase, K. Akahane, N. Yamamoto, M. Sasaki, M. Kujiraoka, and K. Ema, J. Lumin. **128**, 1016 (2008).